INTL JOURNAL OF ELECTRONICS AND TELECOMMUNICATIONS, 2010, VOL. 56, NO. 3, PP. 301-306
Manuscript received July 10, 2010: revised September, 2010. DOI: 10.2478/v10177-010-0040-1

Time Correlated Single Photon Counting System for Optical Measurements

Artur Trybuła, Grzegorz Domański, Bogumił Konarzewski, Janusz Marzec, Krzysztof Zaremba, Robert Kurjata, Michał Dziewiecki, Andrzej Smolnik, and Marcin Ziembicki

***Abstract*—The high sensitivity time correlated single photon counting system (with photomultiplier tube) for biomedical measurements was designed and tested. Photon time of flight through a parafine wax phantom was modeled by Monte Carlo simulation and next measured by the device. Mean time delay introduced by a phantom is in a good agreement with simulation results. The results presented in this paper demonstrate the feasibility of measuring the optical response with the device.**

***Keywords*—Time correlated single photon counting, photomultiplier tube, optical techniques.**

I. Introduction

OPTICAL tomography is a quite well established method for medical and biological imaging, especially for functional imaging [3]. Visible light and near-infrared (NIR) light interact with biological tissue in absorption and scattering processes. There are many physiologically interesting molecules, which have characteristic absorption spectra at these wavelengths.

Unlike X rays, near infrared photons do not cause tissue damage. The main stream of progress in optical tomography field has focused on developing time of flight devices, which can measure time response of examined objects. In biological and medical measurement, the differing absorption characteristics of oxy- and deoxy- haemoglobin in this wavelength range can then be exploited to yield information about spatial variations in oxygenation and blood volume deep within the tissue. The distinctive scatter properties of tissues such as tumors, gray matter and white matter in the NIR range also provide diagnostic information. NIR techniques can be used to monitor the progression of conditions and potentially allow new treatments to be developed, and the response to treatment to be monitored. Detecting abnormalities in the function of tissues should allow earlier intervention than most other imaging modalities, which are unable to detect events that do not manifest as a gross change in tissue structure or composition. Optical technique offers a number of important advantages over both MEG and fMRI, both of which involve the use of large, heavy, and expensive equipment. Often, an entire portion of a building must be dedicated to these measurements, since elaborate magnetically shielded enclosures must be constructed to both shield the equipment from ambient magnetic fluctuations and in certain cases (high-field MRI) to protect the outside environment from the emanation of stray magnetic fields. Both MEG and fMRI also require that the subject remains motionless to within the order of a voxel over the duration of the experiment, or else spatial resolution could be severely compromised. This makes both MRI and MEG measurements of uncooperative subjects (animals and infants, for example) nearly impossible without pharmacologic intervention. Although anesthesia will render a subject motionless for many hours, it can also severely affect normal neural function, while making voluntary response measurements nearly impossible.

Breast imaging using NIR light would reveal information about the functional, absorbing and scattering properties of suspicious lesions. Current breast screening and diagnostic techniques are either invasive, uncomfortable or provide little specificity. Optical tomography offers the opportunity to identify the nature of a lesion without the need for compression of the breast or the use of ionizing radiation or biopsy. Arm imaging allows the efficacy of optical tomography methods to be evaluated since functional changes in the arm can be readily induced and its size is similar to that of an infant's head.

Creating an imaging system that uses NIR light is not straightforward due to the scattering properties of tissue. Because the light quickly becomes diffuse as it traverses tissue, it is not possible to deduce the internal absorbing structure by simply looking at a number of projections (as is the case in x-ray imaging).

Time correlation single photon counting can be used in time of flight measurement, especially in optical tomography [1, 4]. In this work a system for photon time of flight measurement by means of photon counting was developed.

II. Theory

Photon propagation in turbid media can be approximately described by diffusion equation, which in infinitive homogenous media with radial symmetry takes form [5]:

$$\frac{1}{cD}\frac{\partial \Phi}{\partial t} - \frac{\partial^2 \Phi}{\partial r^2} - \frac{2}{r}\frac{\partial \Phi}{\partial r} + \frac{\mu_a}{D}\Phi = \frac{S_0 \delta(r,t)}{D}, \qquad (1)$$

where:
r - distance from a source, t - time, c - speed of light, Φ - photon fluence rate, μ_a - absorption coefficient, D - diffusion constant, μ_s - scattering coefficient, g - scattering anisotropy coefficient, S_0 - energy of light pulse, δ - Dirac delta function.

A. Trybuła, G. Domański, B. Konarzewski, J. Marzec, K. Zaremba, R. Kurjata, M. Dziewiecki, A. Smolnik, and M. Ziembicki are with Institute of Radioelectronics, Warsaw University of Technology, Nowowiejska 15/19, 00-665 Warsaw, Poland (e-mail: {A.Trybula; G.Domanski; B.Konarzewski; J.Marzec; K.Zaremba; R.Kurjata; M.Dziewiecki; A.Smolnik; M.Ziembicki}@ire.pw.edu.pl).

Relation between diffusion constant and the other optical parameters is given by:

$$D = \frac{1}{3\left(\mu_a + \mu_s(1-g)\right)}. \tag{2}$$

The solution of equation (1) is [4]:

$$\Phi(r,t) = \frac{cS_0}{\left(4\pi Dct\right)^{3/2}} \exp\left(-\frac{r^2}{4Dct} - \mu_a ct \right). \tag{3}$$

Full physical model of photon transport in media requires Monte Carlo simulation [6]. The block schema of simple Monte Carlo program for photon migration in infinitive media is shown in the Figure 1. At the start of the program all variables are initialized and new photon is launched. Its starting position is, for example, vector *(x=0, y=0, z= 0)*. The direction of photon move is sampled from isotropic distribution. Then distance *s* to interaction point is sampled from the formula:

$$s = \frac{1}{\mu_a + \mu_s} \ln \xi, \tag{4}$$

where:
ξ is random variable with uniform distribution in the range *(0, 1)*. The photon is moved from its starting position *(x, y, z)* to the new one *(x', y', z')*:

$$\begin{aligned} x' &= x + s\mu_x \\ y' &= y + s\mu_y \\ z' &= z + s\mu_z \end{aligned}, \tag{5}$$

where:
(μ_x, μ_y, μ_z) - the direction of photon move. Internal photon time is increased by:

$$t' = t + \frac{s}{c}. \tag{6}$$

After photon is moved, a kind of interaction: absorption or scattering, is sampled.

The probability of absorption P_a is equal $\frac{\mu_a}{\mu_a + \mu_s}$ and probability of scattering is *1- P_a*. If scattering is sampled then the new photon direction of move is calculated from:

$$\begin{aligned} \mu'_x &= \frac{\sin\theta}{\sqrt{1-\mu_z^2}}\left(\mu_x\mu_y\cos\varphi - \mu_y\sin\varphi\right) + \mu_x\cos\theta \\ \mu'_y &= \frac{\sin\theta}{\sqrt{1-\mu_z^2}}\left(\mu_y\mu_z\cos\varphi + \mu_x\sin\varphi\right) + \mu_y\cos\theta \\ \mu'_z &= -\sin\theta\cos\varphi\sqrt{1-\mu_z^2} + \mu_z\cos\theta \end{aligned}. \tag{7}$$

Here θ denotes polar angle, calculated from the formula:

$$\cos\theta = \frac{1}{2g}\left\{1 + g^2 - \left[\frac{1-g^2}{1-g+2g\xi}\right]^2\right\}, \tag{8}$$

for *g>0* and from the formula:

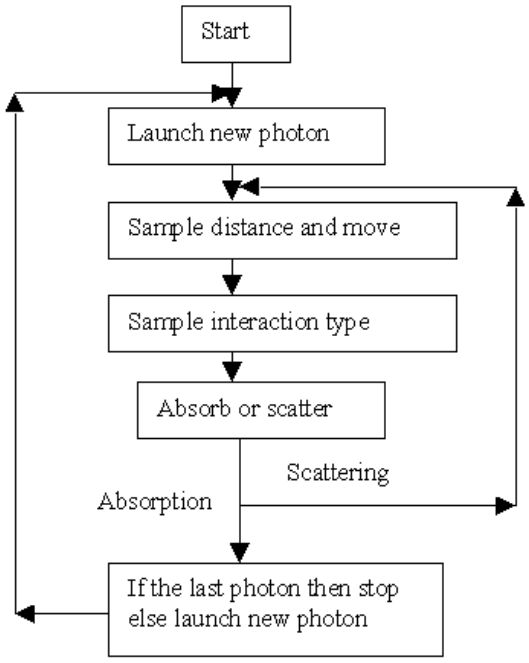

Fig. 1. The block schema of simple Monte Carlo program for photon migration in infinitive media.

$$\cos\theta = 2\xi - 1, \tag{9}$$

for *g=0*.

In the above equations ξ denotes a random variable with uniform distribution in the *(0, 1)* range. Azimuth angle φ is sampled form the uniform distribution in the *(0, 2π)* range. When absorption is sampled then the photon position is checked. If it is in the *(r, r+dr)* range, where *r* is source-detector distance and *dr* is the width of detection layer, the number of detected photon is increased by one in the corresponding time bin.

III. Designed Time Correlated Single Photon Counting System

The high sensitivity time correlated single photon counting system for biomedical purposes was designed and tested. The block schema of developed system is shown in the Figure 2.

Light photons emitted from the source, after transmission through an examined object (phantom), are detected by photomultiplier tube. The system measures the time interval between photon emission moment (START signal) and photon detection moment (STOP signal). Every count is added to the time interval histogram, which creates time response curve.

Laser sources with very short pulses were not available for the authors, so a generator of short light pulses, with duration length about 1 ns, based on LED diode (wavelength 660 nm), was made in our laboratory. It was an inexpensive compact nanosecond LED pulser, proposed by J. S. Kapustinsky and his colleagues [2]. The pulser is based on a fast discharge of a small capacitor via a complementary pair of RF transistors. One of the most important advantages of the pulser is a

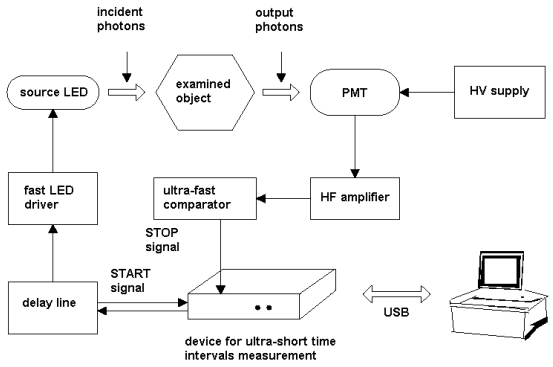

Fig. 2. The block schema of developed time single photon counting system.

possibility to easily adjust the light pulse intensity of LEDs by varying a power supply voltage in contrary to other pulsers based on avalanche transistors where changing amplitude of light pulses in a wide range is more complicated. This pulser provides high performance, simplicity, convenience, and robustness.

In the above system current pulses from photomultiplier tube (PMT) were converted into voltage pulses in wide-band amplifier. Voltage pulses were fed to an ultra-fast comparator, which produced short digital pulses (created by fast PECL logical circuits). These pulses served as STOP signals, which entered one of inputs of ultra-fast time-to-digital converter (TDC).

Time-to-digital converter was TDC-GP2 chip, produced by Acam. Digital TDCs use internal propagation delays of signals through gates to measure time intervals with very high precision. Intelligent circuit structures, redundant circuitry and special methods of layout on the chip make it possible to reconstruct the exact number of gates passed by the signal. Measurement range of this chip is from 3.5 ns to 1.8 µs (0 to 1.8µs between stop channels). Its theoretical time resolution was about 50 ps rms.

A START signal, that controlled LED driver and entered the second input of the TDC, was produced by microcontroller.

The Hamamatsu fast PMT type R6350 (13 mm diameter, 9-stage, side-on type) was used as photon detector. This tube has spectral response from UV to visible light (180 nm to 650 nm) and typical rise time 1.4 ns. The tube photocathode was Sb-Cs. The modular construction of the device, in particular high voltage PMT supplying module, is visible in the block schema.

The system was controlled by fast 32-bit ARM embedded microcontroller type LPC2106, which communicated to PC computer by Universal Serial Bus.

A photograph of the complete system with details of mechanical construction is shown in the Figure 3. PMT module, as well as examined object, was enclosed in light tight brass box.

The acquisition and control program was written in C++ language. The program enables data reading from the device and control high voltage supply of the PMT and of the comparator threshold. The main window of the program was shown in the Figure 4.

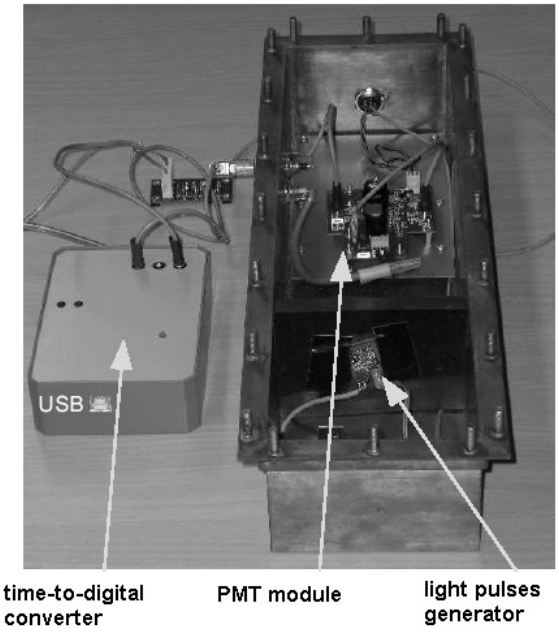

Fig. 3. Complete system for time of flight measurement.

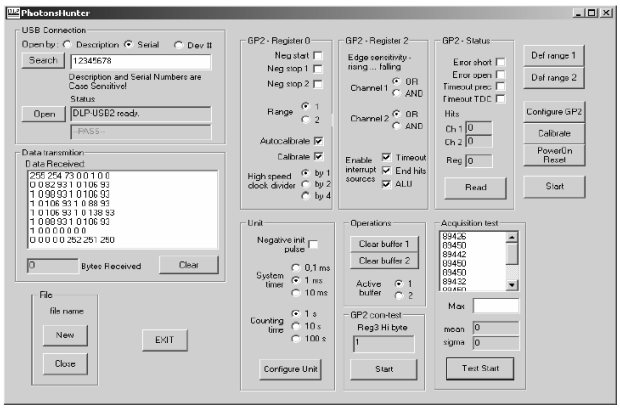

Fig. 4. The main window of the acquisition program.

IV. The Results of Analytical Calculation and Monte Carlo Simulations

Theory presented earlier was applied to analytical calculations of time response for various optical parameters.

For fixed light absorption coefficient μ_a=0.05 cm^{-1}, the tree values of light scattering coefficient were used: μ_s =0.5 cm^{-1}, μ_s =1.0 cm^{-1}, μ_s =2.0 cm^{-1}. Values of other parameters were: g=0, n=1.47. The results of computations are shown in the Figure 5.

Amplitude of time response decreases with increasing of light scattering coefficient. Peaking time is increased with increasing scattering coefficient.

For fixed light scattering coefficient μ_s =1.0 cm^{-1}, the tree values of light absorption coefficient were used:μ_a=0.025 cm^{-1}, μ_a=0.05 cm^{-1}, μ_a=0.1 cm^{-1}. Values of other parameters were: g=0, n=1.47. The results of computations are shown in the Figure 6.

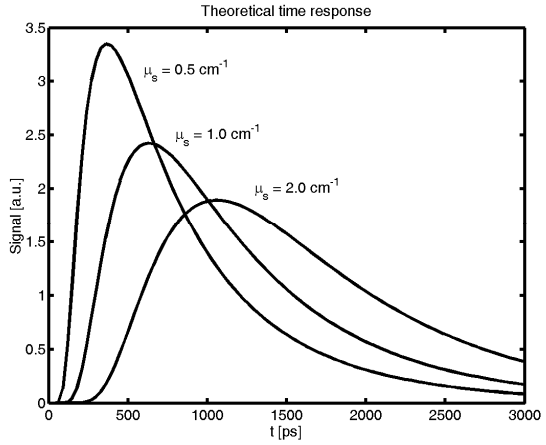

Fig. 5. Theoretical time response for various light scattering coefficient.

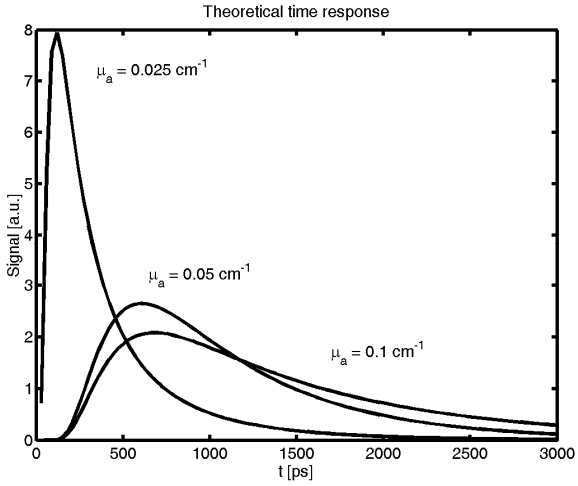

Fig. 6. Theoretical time response for various light absorption coefficient.

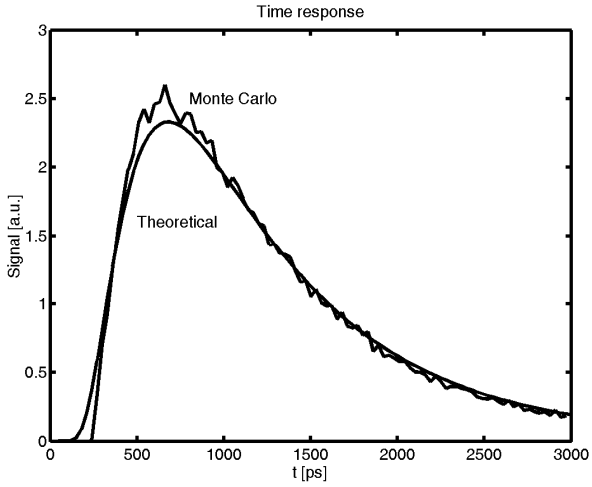

Fig. 7. Theoretical and simulated by Monte Carlo method time response.

Amplitude of time response decreases with increasing of light absorption coefficient. Peaking time is increased with increasing absorption coefficient.

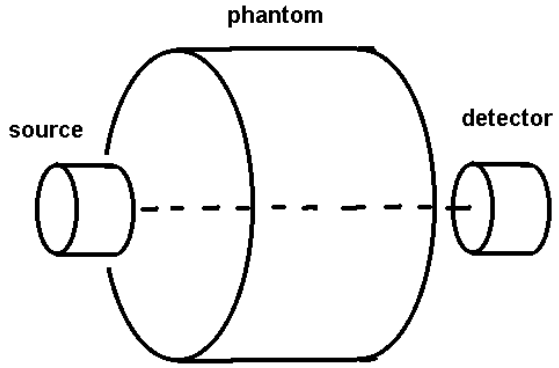

Fig. 8. The geometry of the time of flight measurements for paraffin wax cylinder phantom (height 5.7 cm).

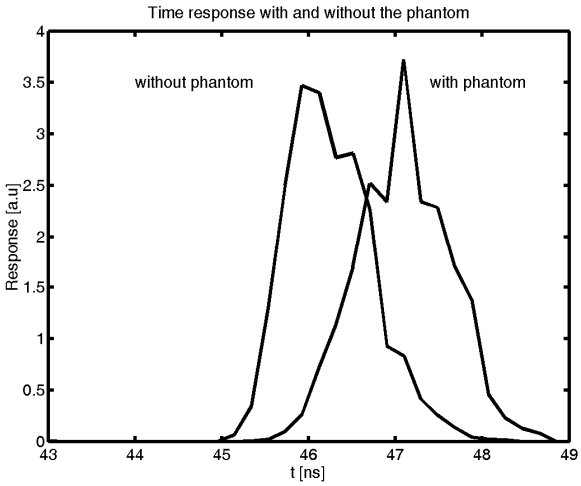

Fig. 9. Measured time response with and without a phantom.

The another simulation was done with the following parameter values: μ_a=0.04 cm^{-1}, μ_s =1.1 cm^{-1}, g=0, n=1.47. These values were chosen by measurement of optical parameters by means of dc signal amplitude [3]. The combination of such values of μ_s =1.1 cm^{-1} and g=0 was used instead of unknown value of μ_s and g, which yields the same value of reduced scattering coefficient *(1-g)* μ_s. The number of simulated photons was 2000000. Theoretical time response curve was calculated from the equation (1). Both time responses: theoretical and simulated were shown in the Figure 7.

A quite good fit between theory and Monte Carlo simulation is visible.

V. The Results of Device Tests

The time response distribution was measured for two cases: with and without a paraffin wax phantom. The phantom was cylindrical: height was 5.7 cm and radius was 3.15 cm. The light source was located on the phantom axis as well as the detector. The measurement geometry is shown in the Figure 8.

Measured time response with and without a phantom is shown in the Figure 9. Delay line was used in the measurement system, so there was the shift about 44 ns in time axis. Only

time differences between two responses: with and without phantom are important.

These experimental results were confirmed by both Monte Carlo simulation and analytical calculation. The tests of developed device confirmed its usefulness for single photon counting measurements.

There is clearly visible the time shift (of order 0.8 – 0.9 ns) between two time responses: with and without paraffin wax phantom. The predicted from simulations first moment shift in the distribution (mean time) is approximately 0.8 ns.

Fluctuations in the curves are caused by poor photon counting statistics.

VI. Conclusions

Analytical computations, based on simplified diffusion theory, were made, as well as Monte Carlo simulation. The results of the computations confirmed that time response curve depends on optical parameters of examined object. It enables determination light scattering and absorption coefficients by time of flight measurements.

The digital TDC-GP2 chip seemed to be very suitable for time correlated single photon counting system. Its time resolution is sufficient for assumed precision in optical systems.

The experimental results presented in this paper demonstrate the feasibility of measuring the optical response with the device. The device parameters are sufficient for noninvasive optical parameters of tissue measurement.

References

[1] E. M. C. Hillman, J. C. Hebden, M. Schweiger, H. Dehghani, F. E. W. Schmidt, D. T. Delpy, and S. R. Arridge. “Time resolved optical tomography of the human forearm”, *Physics in Medicine and Biology*. vol. 46, 2001, pp. 1117–1130.

[2] J.S. Kapustinsky et al, *Nuclear Instruments and Methods A*, vol. 241, 1985, p. 612.

[3] A. B. Milstein, “Three-dimensional optical diffusion tomography with experimental data”, *Optics Letters*, vol. 27, no. 2, 2002, pp. 95-97.

[4] F. E. W. Schmidt, M. E. Fry, E. M. C. Hillman, J. C. Hebden, and D. T. Delpy, “A 32-channel time-resolved instrument for medical optical tomography”, *Review of Scientific Instruments*, vol. 71, no. 1, Jan. 2000.

[5] A. Trybuła, G. Domański, B. Konarzewski, J. Marzec, and K. Zaremba, “System do pomiaru czasu przelotu fotonów przez tkankę”, *Elektronika* vol. 11, 2009, pp. 143-145, [in polish].

[6] L. Wang, S. Jacques, and L. Zheng, “MCML – Monte Carlo modeling of light transport in multi-layered tissues”, *Computer Methods and Programs in Biomedicine*, vol. 47, 1995, pp. 131-146.